

Machine-Learning Discovery of Highly Oxidized IrO_x Phases

Raul A. Flores,^{*,†} Christopher Paolucci,^{*,‡} Ankit Jain,^{*,¶} Muratahan Aykol,^{*,§}
Jens K. Nørskov,^{*,¶} Michal Bajdich,^{*,||} and Thomas Bligaard^{*,||}

[†] *SUNCAT Center for Interface Science and Catalysis, Department of Chemical
Engineering, Stanford University, Stanford 94305, California, USA*

[‡] *Department of Chemical Engineering, University of Virginia, Charlottesville, Virginia
22903, United States*

[¶] *Department of Physics, Technical University of Denmark, Lyngby, Denmark*

[§] *Toyota Research Institute, Los Altos, CA 94022, USA*

^{||} *SUNCAT Center for Interface Science and Catalysis, SLAC National Accelerator
Laboratory, Menlo Park, CA 94025, USA*

E-mail: flores12@stanford.edu; cp9wx@virginia.edu;

temp_temp_ankits_email_address_temp_temp@dtu.dk; muratahan.aykol@tri.global; jkno@dtu.dk;

bajdich@slac.stanford.edu; bligaard@stanford.edu

Abstract

Recent advancements in statistical methods, colloquially termed as machine learning, have revolutionized a tremendous number of fields due to the ease by which we can train models that are flexible enough to regress to data of interest while maintaining predictive power. Nowhere has this impact been felt as much as in the field of materials science, which had previously been bottle-necked by relatively computationally expensive methods. Herein, we report on a ML methodology to enumerate bulk

crystal structures in the IrO_2 and IrO_3 space.

Introduction

TEMP — iaajfsdjdifsdugsdfa — TEMP Iterative Active Machine Learning and unique prototype identification to discover stable new materials and catalysts. Motivation for IrO_x , low representation, longstanding controversy over oxidation states and topology, and demonstrates promise for OER and Li ion batteries.

Reported +6 oxidation state phases are achievable leading to high degree of structural variability, which is the highest for transition metals. High oxidation states (low pH high anodic voltage, harsh oxidizing conditions) unexplored, need very specific structures with precise oxygen connectivity (aka high pressure SrIrO_3) that can exist. Machine learning is the efficient way to explore this “exploring Antarctica for life” sparse space. What we show here...

Crystallographic Discovery and Machine Learning. Current state of databases (OQMD, MP, CatHub, alflowlib). What parts of the database are missing (e.g. IrO_3). Ankit - Condensed version of Ankit paper Prototyping databases to identify knowledge gaps. Deriving features from structures to describe heats of formation. What has been done (simple models) more recently using DFT+Machine Learning.

Oxides for batteries/fuel cells, Iridium Oxide, OER, Lithiated IrO_3 . Highly oxidized phases of oxides for fuel cell and energy storage applications.

Results and discussion

I. IrO_2

For Structure Rendering Use: @Michal To Send example vesta files, font Avenir

Figures: Summary figure of found structures, - There are XYZ unique AB2 structures (or

multiples, e.g. A2B4) - Of those we found 697 unique AB2 prototypes (unique SG/Wyckoff combination) in OQMD/MP - To generate our test set we substituted Ir for A and O for B, then isotropically expanded cell volume to constrain a minimum Ir-O distance of XYZ
 - Next translated each of the 697 structures to be described by 271 features (invariant to isotropic expansion/compression), then reduced to 30 using PCA, described in methods XYZ
 - To generate initial training data use existing DFT. Not enough on IrO₂, so used OQMD to generate initial training data from nearest structures in phase space, described in Methods XYZ. Training set of 30 structures in SI XYZ.

- Trained Gaussian Process, rational quadratic kernel, variable length scales. CV error of XYZ eV/atom, initial predictions in figure XYZ. - Selected 10 structures with lowest prediction-uncertainty for DFT. Structures were volume optimized, then fully relaxed, described in methods XYZ. - Model retrained with the 10 DFT computed structures ONLY, 271 features-110 features applicable to IrO₂-20 principle components for 99.9 percent variance. CV error... - Repeat until XYZ, final predictions shown in Fig XYZ

- Describe relevant features - Physical intuition? - Describe convex hull plot (energy vs. Ir-O distance), computed amorphous phase to define synthesizability - While only 2 IrO₂ in MP/OQMD, we can compare our structures to other computed IrO₂ not in open databases.

This is a citation example.¹ Without it I think stuff breaks.

II. IrO₃

- XYZ unique AB3 Structures, 259 unique prototypes. Substitute Ir and O, expand to minimum Ir-O distance 1 XYZ - followed same procedure as in 3.1, Training Set of 35 structures, 8 of which are IrO₃ - Describe initial training and training after first 10 DFT structures

- Describe convex hull, classes of structures (α -AlF₃ like, rutile like, and layered, should be segregated in hull plot) - briefly describe structures within each class, cite in literature where appropriate

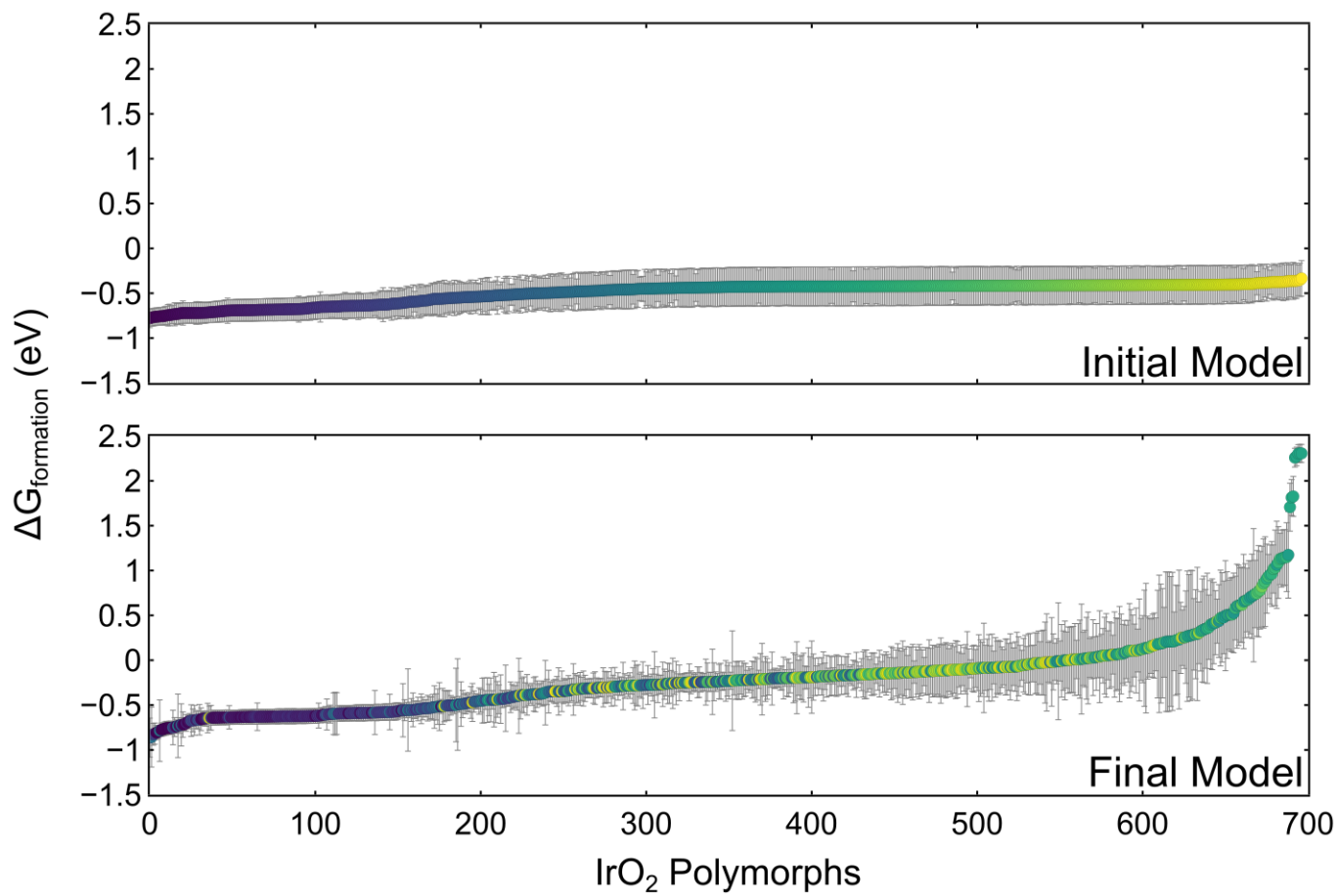


Figure 1: TMP.

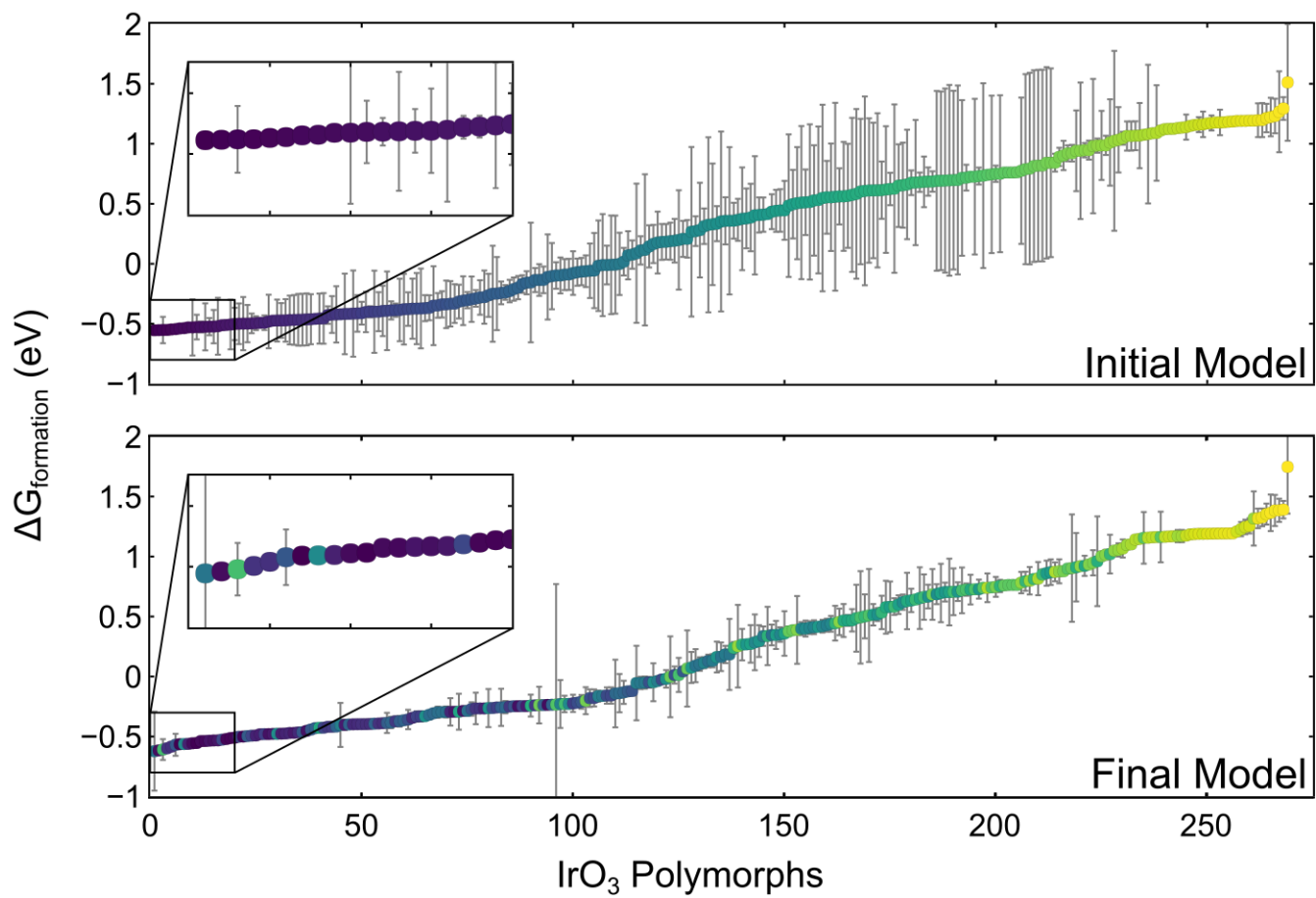


Figure 2: TMP.

III. Electrochemical OER Application

In the following section we will demonstrate the merit of our bulk crystal searching method by investigating the 4 most stable structures for the oxygen evolution reaction, an important electrochemical reaction with application in energy storage technologies.

Bulk Pourbaix

The electrochemical stability phase diagram (E vs. pH) was constructed from all bulk crystals of Ir, IrO₂, IrO₃, and aqueous dissolved IrO₄[4-]. Only the most stable structure for each stoichiometry is visible on the Pourbaix diagram which correspond to TEMP and are shown in Fig. 3

Under acidic condition (i pH 7) and in the bias region of of interest for the OER, there exists a region of stability for the novel α -AlF₃ IrO₃ structure found herein.

At a pH=0 the bound of stability for α -AlF₃ IrO₃ spans TEMP

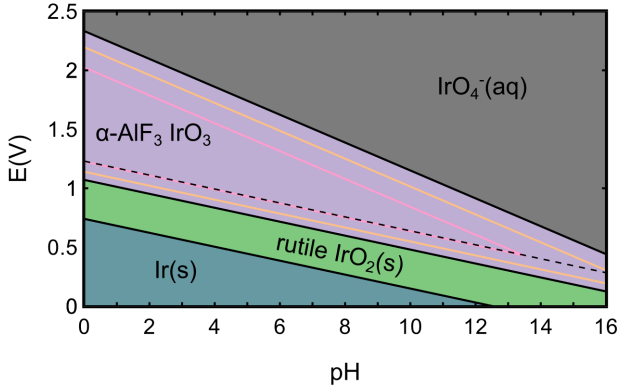


Figure 3: Electrochemical bulk phase stability diagram (Pourbaix) of the Ir-O-H chemical space.

b. OER Activities and Surfaces

The OER activity (expressed in over-potential) for surfaces cut from the IrO₂, and the 3 most stable polymorphs of IrO₃ are shown in Fig. 4. The specific facets were chosen from

the highest intensity x-ray diffraction peaks from powder-diffraction spectra simulated in VESTA.

To determine the most likely experimentally abundant surface facets and surface coverages, a surface energy Pourbaix diagram was constructed (TEMP). See (SI for surface energy/Pourbaix part) for the method used to calculate surface energies.

c. OER Intermediate Scaling

Write stuff

Conclusion

And in conclusion we presented work here...

Acknowledgement

Organizations to acknowledge TRI SUNCAT Stanford NERSC etc.

JAGT and MB acknowledge the support by the U.S. Department of Energy, Office of Science, Office of Basic Energy Science, via Grant DE-SC0008685 to the SUNCAT Center of Interface Science and Catalysis.

The authors would like to acknowledge the use of the computer time allocation for the “Transition metal-oxide and metal surfaces: applications and reactivity trends in catalysis” at the National Energy Research Scientific Computing Center, a DOE Office of Science User Facility supported by the Office of Science of the U.S. Department of Energy under Contract No. DE-AC02-05CH11231.

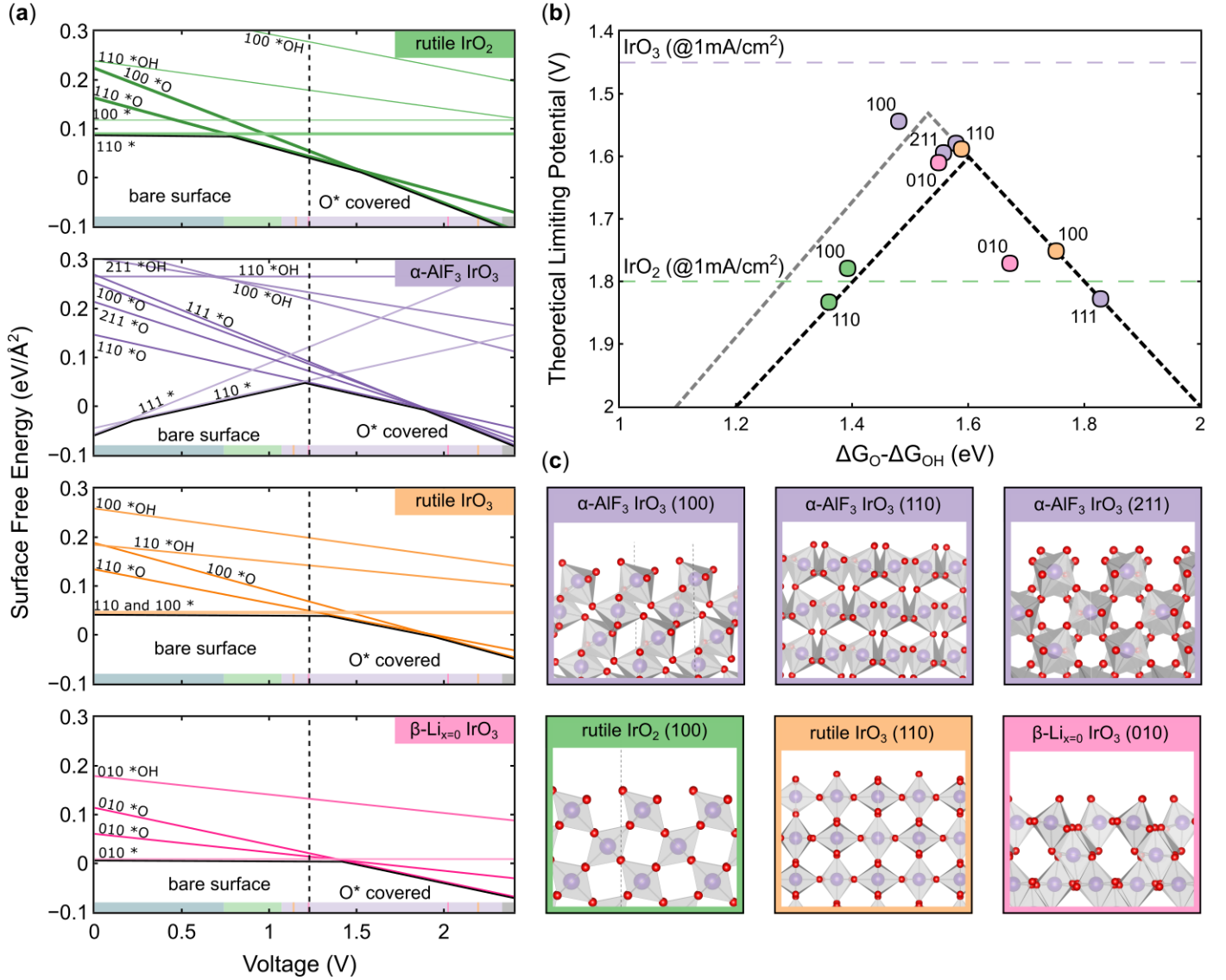


Figure 4: Summary of OER results for the four bulk structures of IrOx considered: rutile-IrO₂ (green), α-IrO₃ (purple), rutile-IrO₃ (orange), and b-IrO₃ (pink). (a) Surface energy Pourbaix diagrams for each structure, with the surface energy of various facets and coverages shown as a function of applied potential. The bulk Pourbaix diagram's bounds of stability at pH 0 are superimposed at the bottom of each subplot. (b) OER activity volcano for IrOx systems considered. Circles designate oxygen covered surfaces while triangles designate hydroxyl (*OH) terminated surfaces (relevant surface terminations were found via surface Pourbaix analyses). Surface energies at standard conditions (pH and V = 0) are reflected in the border color for each data point, where black indicates a low energy surface termination and white indicates more unstable surfaces. (c) Select surface structures for IrOx systems considered herein.

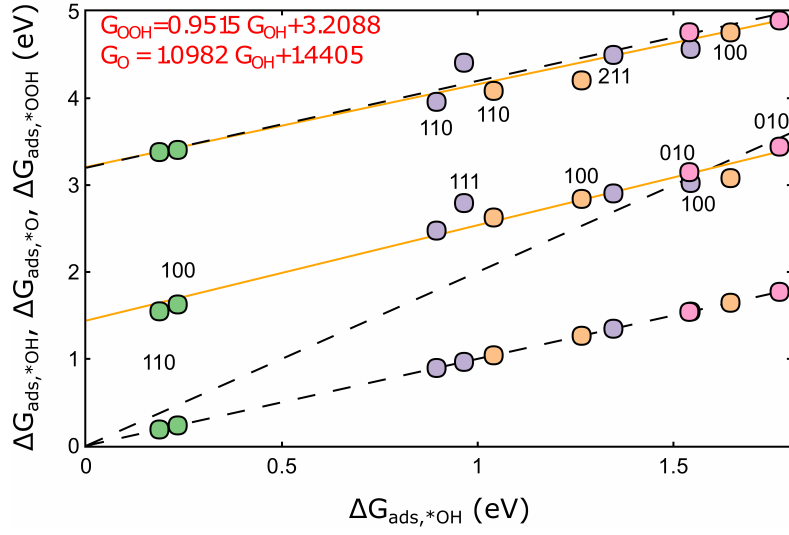


Figure 5: Scaling relationship between DG of adsorption of the intermediate species of the OER using $\Delta G_{\text{ads},*OH}$ as a descriptor. $\Delta G_{\text{ads},*OOH}$, $\Delta G_{\text{ads},*O}$, and $\Delta G_{\text{ads},*OH}$ are plotted on the y-axis.

Supporting Information Available

Machine Learning Algorithm Methods

Relevant details about the ML Gaussian process here

Electrochemical OER Computational Methods

Density Functional Theory Methods

All OER calculations were performed using density functional theory (DFT) implemented via the Vienna ab-initio simulation package (VASP) and utilizing the PBE exchange-correlation functional. Dipole corrections were imposed on all non-symmetric slabs. A 4x4x3 k-point mesh with gamma-point centered Monkshort-packing was used for all slabs. The plane-wave energy cutoff was 500 eV.

All slab calculations maintained a vacuum spacing of 15 Å. All structures were relaxed utilizing a TEMP algorithm with a stop criteria being that all atoms satisfy a maximum force threshold of 0.02 eV/Å.

OER Thermodynamic Methodology

Surface Energy Pourbaix Methodology

Procedure: - For the top/most stable bulk structures the following procedure was carried out

- * Stable stoicheometric terminations were cut from the bulk Stable termination planes were guesstimated via intuition, and the x-ray diffraction pattern tool from Vesta

- * Electrochemical surface coverage was elucidated via a surface Pourbaix analysis Need to know the coverage of surface under operating conditions (1.23 V RHE)

- * Thermodynamic/limiting potential analysis of the OER mechanistic pathway Volcano plot, limiting potentials, etc.

References

- (1) Smith, A.; Smith, J. TEMP title. **9999**, *1*.

Graphical TOC Entry

